NUMERICAL COMPARATIVE STUDY OF BPM DESIGNS FOR THE HESR AT FAIR

A. J. Halama, C. Böhme, V. Kamerdzhiev, F. Klehr, S. Srinivasan
Forschungszentrum Jülich, Germany

Abstract

The Institute of Nuclear Physics 4(IKP-4) of the Research Center Jülich (FZJ) is in charge of building and commissioning the High Energy Storage Ring (HESR) within the international Facility for Antiproton and Ion Research (FAIR) at Darmstadt. Simulations and numerical calculations were performed to characterize the beam position pickup design that is currently envisaged for the HESR, i.e. a diagonally cut cylindrical pickup. The behavior of the electrical equivalent circuit has been investigated with emphasis on capacitive cross coupling. Based on our findings, performance increasing changes to the design were introduced. A prototype of the BPM pickup was constructed and tested on a dedicated test bench. Preliminary results are presented. Another proposed design was characterized and put into comparison, as higher signal levels and higher position sensitivity are expected. That is a symmetrical straight four-strip geometry. Additionally an extensive study was conducted to quantify the effect of manufacturing tolerances. Driven by curiosity an eight-strip pickup design was considered, which would allow for beam size measurements, utilizing the non-linearity.

CAPACITIVE PICKUPS

Capacitive pickups are widely used in particle accelerators as intensity and position monitors. Being non-destructive devices these pickups are of great interest especially in ring accelerators and those where beam may not be lost. Capacitive pickups such as the cylindrical diagonally cut electrodes facilitate the image current, which is influenced by the beam with close resemblance to a perfect current source, as it is mostly modelled in the equivalent circuit. Its pulse shape is given by the time derivative of the longitudinal beam recorded at the pickup location. As a design choice for the HESR the voltage of an electrode shall reflect the longitudinal time structure proportionally. For this case the main frequency contribution of the signal must lie above the cut-off frequency of the RC couple. This is achieved by the high input impedance of the attached preamplifier. The voltage of a centered beam is [1]:

$$U_{img}(t) = \frac{1}{\beta c C_{el}} \frac{A}{2\pi b} I_{beam}(t) \tag{1}$$

With β:=normalized velocity, c:= speed of light, A:= electrode inner surface area and b:= BPM radius. If at least two opposing electrodes are used, a linear response of the voltage versus the beam position can be seen in the centre region of nonlinear BPM such as strip types or buttons. Whereas the cylindrical diagonally cut BPM offers a linear response in the entire region. The linear response can be generalized as the normalized difference signal. Thus the difference over sum ratio is used to describe the linear behaviour [1][2]. For x and similarly y, with S being the sensitivity:

$$x = \frac{1}{S_x}\frac{U_r - U_l}{U_r + U_l} - x_{off} = \frac{1}{S_x}\frac{\Delta_x}{\Sigma_x} - x_{off} \tag{2}$$

To account also for higher order behaviour, ether a lookup table or use a two-dimensional polynomial can be used. For x and similarly y:

$$x = \sum_{i=1}^{N}\sum_{j=1}^{N} K_{x,ij}\left(\frac{\Delta_x}{\Sigma_x}\right)^i\left(\frac{\Delta_y}{\Sigma_y}\right)^j \tag{3}$$

Simulation Boundary Conditions and Formalism

An equivalent circuit has been used to model the voltage response driven by a current source. The circuit evaluation for these studies was carried out using LTspice IV.

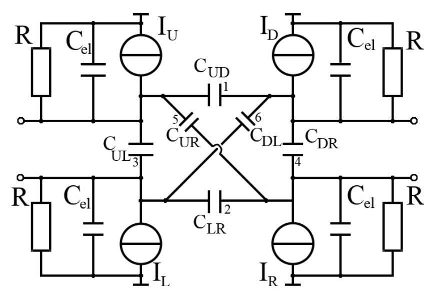

Figure 1: Equivalent circuit of a capacitive four electrode pickup.

For the case of 4 electrodes there are 10 capacitances, i.e. four capacitances against ground, which correspond to C_{el} in Eq. (1). The remaining ones are interconnecting all electrodes, all as illustrated in Fig. 1. The capacitances for the presented results have been determined using COMSOL Multiphysics 5.0 AC/DC analysis, as it allows for static electric field simulations with fixed and floating potentials. The dependence on the beam position is introduced as a geometrical scaling factor, Γ, which would be $\Delta\phi/2\pi$, for a centred beam. It increases for a beam that approaches the electrode. $\Delta\phi$ is the average angular coverage. The scaling factor can be determined for any geometry.

$$\Gamma(\phi_1, \phi_2, r, \theta) = \frac{\int_{\phi_1}^{\phi_2} \frac{l_{BPM}(\phi)}{(\vec{r}_{BPM}(\phi) - \vec{r}_{Beam}(\theta))^2}\,\mathrm{d}\phi}{\int_{0}^{2\pi} \frac{l_{BPM}(\phi)}{(\vec{r}_{BPM}(\phi) - \vec{r}_{Beam}(\theta))^2}\,\mathrm{d}\phi} \tag{4}$$

With θ and $\vec{r}_{Beam}$ pointing at the beam. Eq. (4) has been derived empirically with the intention to reflect the position dependent influence, driven by the electrical field of the

ISBN 978-3-95450-177-9

beam. The integrals can be solved for example for strip type BPMs with a continuous length and a given angular coverage, so $\phi_{1,2} = \mp\frac{\phi_0}{2}$ [2].

$$\Gamma(r,\theta) = \frac{\phi_0}{2\pi}\left(1 + \frac{4}{\phi_0}\sum_{n=1}^{\infty}\frac{1}{n}\left(\frac{r}{b}\right)^n cos(n\theta)sin\left(\frac{n\phi_0}{2}\right)\right) \quad (5)$$

The resulting scaling factor Γ can only be used to describe pencil beams and radially symmetrical beams. For elliptical beams a Gaussian distribution can be applied. Using this toolset, response maps of the electrode voltages, difference over sum ratios and sensitivity distributions can be obtained to characterize BPM types and geometries.

Diagonally Cut BPM

The chosen design for HESR BPMs at the current stage is the cylindrical diagonally cut BPM [3], as it offers high reliability due to its linear response. It is shown in Fig. 2

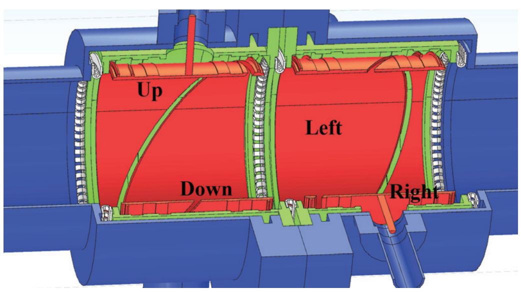

Figure 2: Cut view on diagonally cut BPM model, red: electrodes, green: grounded housing, blue: beam pipe.

Using COMSOL, a simplified model of the BPM with housing cylinder and surrounding beam pipe has been modeled in accordance with the CAD model. With simulated capacitances plugged into Eq. (1), the expected output voltage was calculated and compared to thermal noise levels. The beam conditions were taken as: $10^8\ \bar{p}$, $T_{kin} = 3$ GeV and $l_{bunch} = 150$ m. The initial design has been modified to reduce C_{el} and enhance thereby the signal strength. These changes were: shortening screws to the mechanically necessary length, widening the feedthrough hole in the housing cylinder, chamfering edges, removing mechanically unnecessary pieces, increasing the cut from 2 mm to 3 mm and increasing the distance of the electrode to the housing cylinder. According to simulation results, these changes lowered the capacitance against ground by approximately 25 %. Regarding the capacitances, the latest simulation results are shown in table 1. Subscripted numbers indicate the location in Fig. 1.

Given these results and the dimensions of the BPM, the voltage for a centred beam at each electrode with estimated capacitances of the feedthrough and preamplifier is 275 μV for the upper and right electrode, and 280 μV for the bottom and left electrode. The sensitivity in the centre region is 1.36 %/mm in both planes. The capacitances against ground are different for electrodes located closer to the centre, which causes an measured position offset. The cross electrode

Table 1: Simulated Capacitances, Diagonally Cut BPM

Port A	Port B	Capacitance$_{AB}$ [pF]
Up or Right	GND	17.44
Down or Left	GND	16.73
Up_1/ $Left_2$	$Down_1$/ $Right_2$	5.84
Up_3/ $Down_4$	$Left_3$/ $Right_4$	0.104
$Down_5$	$Left_5$	0.658
Up_6	$Right_6$	0.021

capacitances are distributed asymmetrically. This introduces a slight tilt of the linear response plane, causing crosstalk and a slightly position dependent sensitivity. The last two effects can only be seen with high resolution, as for example the simulation allows. Under measurement conditions these are mostly negligible. The displacement of the electrical centre is 0.68 mm in x and 0.59 mm in y. These are expectancy values for a flawless BPM.

Comparison of Measurement and Model

A stretched wire test bench has been constructed in the IKP-4 for characterization tests of BPMs. Two pairs of linear drive stages translate a wire as beam analogue, through which a specfic pulse is sent. Optical micrometres assure precise matching of the wire with desired positions. A fast 16bit ADC PCIe-card reads preamplified voltages from the electrodes. Data processing is done via a LabVIEW software. With help of the test bench one was able to confirm signal level expectations for the BPM and measure its sensitivity. The test bench measurement yields a sensitivity of (1.318 ± 0.003) %/mm in one plane and (1.330 ± 0.003) %/mm in the second plane. The electrical centre was measured at the position 0.21 mm vs. 0.94 mm. These results comply well with the expectations. The systematic difference in sensitivity and offset can be explained by manufacturing tolerances. An additional insight will be obtained soon as precise capacitive measurements of the pickup are planned.

Strip Type BPM

The capacitive strip type BPM has been investigated for comparison with expectations of higher signal levels, higher centre sensitivity, symmetric crosstalk conditions, and a small offset from the absolute mechanical centre positon. The capacitances are shown in tab. 2. A model image is shown in Fig. 3

Table 2: Simulated Capacitances, Strip Type BPM

Port A	Port B	Capacitance$_{AB}$ [pF]
Any electrode	GND	17.06
Any electrode	Port A+180°	0.449
Any electrode	Port A±90°	2.211

As one can see, the capacitances for the same geometrical relations are equal. Due to this fact, the unwanted

ISBN 978-3-95450-177-9

features of the diagonally cut design are being circumvented. Space limitations for this geometry are different, therefore it could be longer than the diagonally cut BPM. For a length of 270 mm and an angular coverage of 70°, the electrode voltage for a centred beam is 390 μV. The expected sensitivity is 3.59 %/mm.

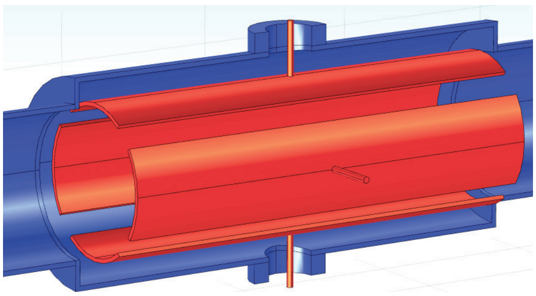

Figure 3: Model image of simplified strip type BPM, red; electrodes, blue; beam pipe.

Misalignment Analysis

To show that the strip type design is robust towards mechanical misalignments an extensive study has been conducted. About 150 models were created with angular and translational misalignments in different error magnitudes. Each electrode has been randomly pitched (1.5°), yawed (1.5°), rolled (4°) and shifted (2 mm) along three axis with the denoted maximum values in parentheses for the maximum error case. RMS deviations between ideal positions and misaligned BPM positions have been calculated. The RMS deviation scaled according to the error magnitude. If individual lookup tables are used, it could be shown, that the misalignments cause less of a disturbing effect than the non-linearity itself. RMS deviations were small at the centre. The analysis showed that any compensation method for the non-linearity would be able to correct for misaligned errors, too. The used misalignments were exaggerated chosen far beyond reasonable manufacturing tolerences. Fig. 4 shows linear projections of an intact and a misaligned BPM, using the linear approximation (Eq. (2)) and centre sensitivity value.

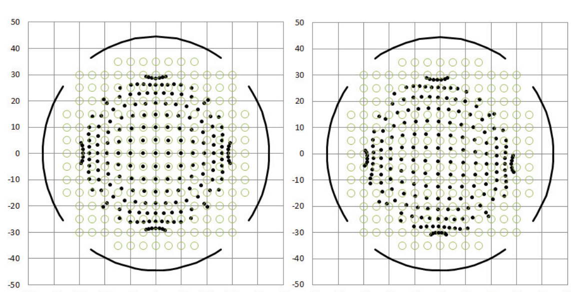

Figure 4: Projection plot of ideal and misaligned strip type BPM.

Disadvantages

Although the strip type BPM outperforms the diagonally cut BPM as expected with a higher signal strength and higher sensitivity, the major disadvantage of the strip type BPM is the non-linear response. So one has to invest into more sophisticated calculation schemes as in Eq. (3). Due to the non-linearity, the measured beam position is dependent on the beam size. An approximate position can still be retrieved with an error. Despite the cross plane capacitance influence the sensitivity map of the diagonally cut BPM is reasonably flat and can be used for beam position determination. Minor adjustments to the coefficients, like adding an (position dependent) offset and a crosstalk term, makes the design still yielding. This BPM shows only little dependency towards beam size and makes it thereby a more versatile device and easy to use.

CONCEPT OF BEAM SIZE MEASUREMENT

The size dependency was studies exclusively with transverse Gaussian distributions. Looking at strip type BPMs, it can be shown that Eq. (5) holds only true for pencil beams and beams of equal horizontal and vertical size (i.e. σ_x=σ_y). This is why beam position monitors with linear responses are more preferred to show no or only a little size dependency. The dependency of non-linear pickups can be used to determine the beam size in return with an expanded model and design. For this purpose a simple model of a BPM with eight electrodes has been developed, where only two electrodes are shifted outwards, one in x (2) and the other in y (0) direction.

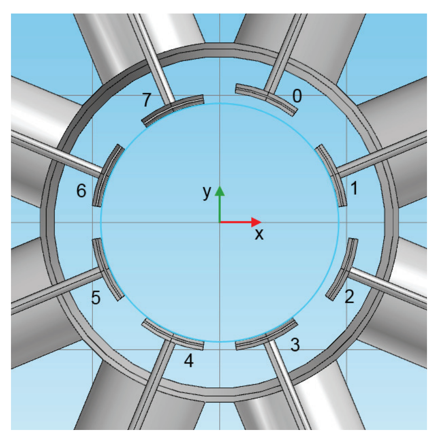

Figure 5: Cross-sectional view on eight strip BPM.

As there are eight electrodes, a specific configuration can be chosen, as which some electrodes act as ‘Up’ electrode, some as ‘Down’ etc. If the coefficient matrix is known, the beam position from the signals on all electrodes can be calculated. As implied before the read position is faulty, if the coefficient matrix has been determined for a pencil beam. To introduce a size relation, each coefficient can be a

ISBN 978-3-95450-177-9

function of beam size in x and y.

$$x = \sum_{i=0}^{N}\sum_{j=0}^{N}\left(\sum_{l=0}^{M}\sum_{m=0}^{M} G_{x,ij\,ml}\,\sigma_x^l\sigma_y^m\right)\left(\frac{\Delta_x}{\Sigma_x}\right)^i\left(\frac{\Delta_y}{\Sigma_y}\right)^j \tag{6}$$

A number of unique configurations have been found that would yield stable and reliable coefficient matrices. Each configuration can be rotated by 45° (i.e. shifting each index by one), mirrored and flipped. This way, up to 16 versions of a single configuration are obtained. Labelling each electrode from 0 to 7 some of these configurations are shown in table 3, enumeration is shown in Fig. 5:

Table 3: Examples for Some Configurations

Up	Down	Left	Right
6,7,0,1	2,3,4,5	4,5,6,7	0,1,2,3
0,7	5,6	0,7	1,2
0,6,7	4,5,6	0,6,7	1,2,3
0,6,7	2,3,4	5,6	1,2

For a given beam that passes through the BPM with a sufficient ellipticity, the beam position can be calculated with an estimated initial beam size (σ_x=σ_y= 0 for simplicity). Taking Eq. (6), each configuration will yield a differing result from the actual beam position, where those do not necessarily coincide. The standard deviation of the estimated beam position is in such a case relatively high. As one approaches the actual beam size the standard deviation decreases and shows its minimum at that spot. If this procedure is continued for an entire sweep through all σ_x and σ_y combinations, one can see that certain combinations of sizes induce the exact same voltage distribution on the electrodes. This can be seen as a valley of minimum standard deviations in a plot over all beam sizes. This is shown in Fig. 6.

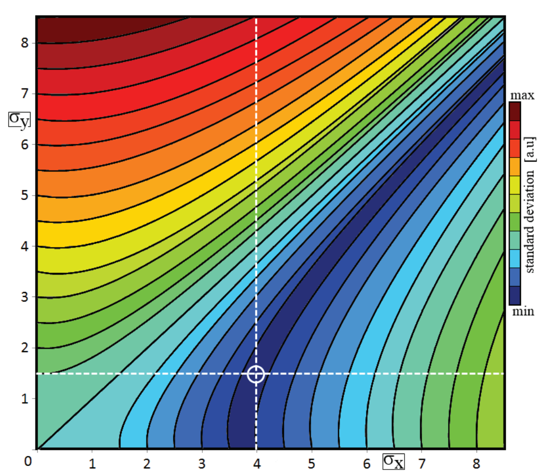

Figure 6: 2D plot of position standard deviation vs. beam size. For beam with dimension σ_x = 4 mm, σ_y = 1.5 mm.

This implies that certain beam sizes are indistinguishable from one another. These isolines can be characterized e.g. for beams with $\sigma_x > \sigma_y$ as in Eq. (7). With c being the axis intersect, a and b as fitting coefficients. If two such beam size monitors are used at locations with zero dispersion, the spot of common emittance, and therefore the actual beam size can be found. The beam size monitors should be located, such that one detects a bigger width in x (Eq. (7)) and the other in y (Eq. (8)).

$$\sigma_{x_1} = \frac{a_1\sigma_{y_1}^2 + b_1\sigma_{y_1} + c_1^2}{\sigma_{y_1} + c_1} = \tilde{f}_1(\sigma_{y_1}) \tag{7}$$

$$\sigma_{y_2} = \frac{a_2\sigma_{x_2}^2 + b_2\sigma_{x_2} + c_2^2}{\sigma_{x_2} + c_2} = \tilde{f}_2(\sigma_{x_2}) \tag{8}$$

$$\sigma_{x,y}\,(s) = \sqrt{\epsilon_{x,y}\beta_{x,y}\,(s)} \tag{9}$$

$$\sigma_{y_1} = \tilde{f}_1\left(\sqrt{\frac{\beta_{x_2}}{\beta_{x_1}}}\tilde{f}_2(\sigma_{y_1})\right)\sqrt{\frac{\beta_{y_1}}{\beta_{y_2}}} \tag{10}$$

With Eq. (10), the beam size can be found, if the equality condition is fulfilled. This is equivalent to finding the axis intersect, $d(\sigma_y) = 0$ in Eq. (11).

$$d(\sigma_{y_1}) = \tilde{f}_1\left(\sqrt{\frac{\beta_{x_2}}{\beta_{x_1}}}\tilde{f}_2(\sigma_{y_1})\right)\sqrt{\frac{\beta_{y_1}}{\beta_{y_2}}} - \sigma_{y_1} \tag{11}$$

$$d(\sigma_{y_1}) \approx -\sigma_{y_1} + e \tag{12}$$

$$e = d(0) = \frac{a_2\frac{\beta_{x_2}}{\beta_{x_1}}c_1^2 + b_2\sqrt{\frac{\beta_{x_2}}{\beta_{x_1}}}c_1 + c_2^2}{c_2 + \sqrt{\frac{\beta_{x_2}}{\beta_{x_1}}}c_1}\sqrt{\frac{\beta_{y_1}}{\beta_{y_2}}} \tag{13}$$

For roughly $\sigma_{x_1} > 3\sigma_{y_1}$ and $\sigma_{y_2} > 3\sigma_{x_2}$, $d(\sigma_{y_1})$ can be approximated as in Eq. (12). The slope in the linear approximation of $d(\sigma_{y_1})$ is about -1, so the beam size at location one is equal to e. From the isoline relations (Eq. (7, 8)) and the emittance relation (Eq. (9)), σ_{x_1}, σ_{y_2}, and σ_{x_2}, as well as ϵ_x and ϵ_y can be calculated.

CONCLUSIONS

The shown analytical studies present a reliable method for the characterization of BPM geometries. A theoretical method for a beam size measurement for elliptical beams and for known size ratios has been presented. The next step will be to construct and test the device.

ACKNOWLEDGEMENT

Thanks to B. Breitkreutz, B. Lorentz, B. Nauschütt, P. Niedermayer, H. Soltner, H. Stockhorst and R. Stassen.

REFERENCES

[1] P. Fork et al., "Beam Position Monitors", CERN Accelerator School 2009, GSI, Germany.

[2] R. E. Shafer, "Beam Position Monitoring", AIP Conference Proceedings 1989, Los Alamos National Laboratory.

[3] C. Böhme, "Beam Position Monitors for the HESR", Annual Report 2014, Forschungszentrum Jülich, Germany.

ISBN 978-3-95450-177-9